An investigation on drought teleconnection with indian ocean dipole and el-nino southern oscillation for peninsular india using time dependent intrinsic correlation

IOP Conf. Series: Earth and Environmental Science **491** (2020) 012007 doi:10.1088/1755-1315/491/1/012007

An investigation on drought teleconnection with indian ocean dipole and el-nino southern oscillation for peninsular india using time dependent intrinsic correlation

Kavya Johny[1,3], Maya L Pai[1] and Adarsh S[2]

[1]Department of Computer Science and IT, Amrita School of Arts and Sciences, Amrita Vishwa Vidyapeetham, Kochi Campus, India.
[2]Department of Civil Engineering, TKM College of Engineering, Kollam, India

Corresponding author – Email: adarsh1982@tkmce.ac.in

Abstract: Drought is an obscure climatic state that has socioeconomic repercussions on power generation, agricultural production, forestry, tourism and construction. In this study, an Ensemble Empirical Mode Decomposition (EEMD) based Time Dependent Intrinsic Correlation (TDIC) analysis was conducted to assess the impacts of Indian Ocean Dipole(IOD) and El Niño-Southern Oscillation (ENSO) to drought events of Peninsular region in India. Standardized Precipitation Index (SPI) at three different time scales (SPI-3, SPI-6 and SPI-12) are considered for analysis. The teleconnections IOD and ENSO on the three indices are evaluated independently using TDIC method and the detection and attribution was made from the obtained correlation plots. From the detailed analysis, short term drought (SPI-3) is found to have better correlation with both IOD and ENSO. It is also interpreted that high frequency modes of SPI-3 have more association to IOD while low frequency modes show more correlation to ENSO. Thereby, IOD experiences a lagged influence on ENSO relation to rainfall. The IMF3 and IMF7 of SPI-12 also show positive association that can be added to existing data for efficient prediction of drought events. Similarly, for ENSO IMF1, IMF6 and IMF7 of SPI-6 and IMF6 and IMF7 of SPI-12 can also be used for determining the drought accurately.

Keywords: Correlation, Drought, Rainfall, TDIC, Teleconnection

1. Introduction

The spatio-temporal distribution of rainfall in the India varies by the global and regional energy flow resulting from many Oceanic-atmospheric interactions. As rainfall is a significant source of freshwater, understanding the link between the individual and combined effects of the drivers at the regional scale is essential. Uneven distribution of rainfall results in recurrent droughts as well as frequent floods in different homogenous regions of India. This natural disaster has strongly impacted agriculture, industry, fisheries, and the daily life of the public.

Standardized Precipitation Index (SPI) [1], Palmer Drought Severity Index (PDSI) [2] and Percent of Normal Precipitation (PNP) [3] Standardized Precipitation Evapotranspiration Index (SPEI) [4] are the meteorological drought indicators used commonly for drought studies. SPI using precipitation is preferred due to its simplicity in estimation and flexibility in temporal scale. Many statistical methods that rely on machine learning techniques and dynamical methods that rely on General Circulation

Models (GCM) have been widely used for drought prediction. In the statistical approaches, the prediction is done based on the empirical relationships between various influencing variables such as temperature, pressure etc. and the physical processes of the ocean, land and atmosphere. The link between these drivers and general hydroclimatic variability has been a focus of several studies. Numerous climatic oscillations like Quasi Biennial Oscillation (QBO), Indian Ocean Dipole (IOD), Atlantic Multidecadal Oscillation (AMO), ElNiño Southern Oscillation (ENSO), Equatorial Indian Ocean Oscillation (EQUINOO) influence rainfall variation [5-9].

Indian Ocean Dipole (IOD) is an ocean-atmospheric phenomenon in which an irregular oscillation of sea-surface temperature occurs [10]. Arabian Sea becomes warmer that enhances atmospheric convection and at the same time, the Bay of Bengal becomes colder causes winds blow from east to west. Vinayachandran et al. [11] studied the various processes and impacts of IOD and stated that the IOD affects rainfall over the Indian subcontinent, eastern Africa and Australia. Bala and Singh [12] tried to establish the relationship between summer monsoon of Kerala and IOD to analyse the rainfall distribution of the country. Johny et al. [13] made an EEMD-based time-dependent intrinsic correlation (TDIC) analyses on IOD and South west monsoon rainfall of Kerala and proved that positive associations are found at localized time spells and dominancy of negative association of IOD in different process scales. Several studies have previously explored teleconnections between ENSO and Indian monsoon rainfall [5, 7, 14-16]. Kripalani and Kulkarni [15] showed that there are more El Niño–related droughts in the decades when the Indian monsoon is generally below normal than during the decades when the Indian monsoon is generally above normal. The teleconnection between ENSO and drought are well described [17-19].

In the past, researchers used several approaches for investigation of hydroclimatic teleconnections at global scale ranging from simple statistical correlation to wavelet based spectral analysis [20-23]. The advanced spectral analysis methods including wavelets and Hilbert Huang Transform (HHT) help to investigate such linkages in multiple time scales. Wavelet analysis is proposed as an efficient alternative for multiscale teleconnection studies of drought indices. Rashid et al. (2019) applied continuous wavelets to analyse SPI for Australia and reported that year to multiyear SPI extremes are strongly related to the low-frequency signal present in climate variables. Inter-annual variability (period of 3.73 and 7.4 years) of climate variables are associated with drought at the annual scale, whereas multiyear droughts are strongly influenced by the variability at interdecadal frequencies (period of 14.9 years). Maity and Nagesh Kumar [24, 25] investigated the link of climatic indices with Indian monsoon using simple statistical correlation. Adarsh and Janga Reddy [26, 27] investigated the teleconnections of different climatic two climate oscillations on the summer monsoon rainfall in India using the multivariate empirical mode decomposition (MEMD) based TDIC analysis. However, no studies used multiscale spectral analysis techniques for investigating the teleconnections between drivers and drought Indices of Indian subcontinent. Hence the the specific objectives of the study are: (1) to investigate multiscale teleconnection between two prominent indexes- ENSO and IOD with SPI of Peninsular India; (2) to find the extremity of the association of variables to short term drought and long term drought.

2. Methods and Materials

2.1. Ensemble Empirical Mode Decomposition (EEMD)

Huang et al. [28] proposed a data adaptive multiscale decomposition method namely Hilbert Huang Transform (HHT) as an alternative to wavelet transform, as the latter one demand *apriori* selection of number of decomposition levels and functional form. The decomposition of the time series will result in a set of zero mean series namely Intrinsic Mode Function (IMF) and a final residue preserving the orthogonal property. The data decomposition operation will be effective only when IMFs are frequency separable. Sometimes an IMF retains the characteristics of more than one frequency content. In such case, complexity arises in the physical interpretation of the signals leading to wrong

conclusions. Different researchers proposed ensemble averaged and noise-assisted variants of EMD to overcome this serious drawback so called 'mode mixing' and one such variant proposed by Wu and Huang [29] called as Ensemble Empirical Mode Decomposition (EEMD). The typical steps of iterative procedure of EEMD are: (i) addition of a white noise series to the given time series signal to form an ensemble of artificial signals; (ii) decompose each artificial signal by EMD to evolve an IMF; (iii) perform ensemble averaging to get the desired IMF. More details on the algorithm can be found elsewhere [29].

2.2. Time Dependent Intrinsic Correlation

The association of two correlated time series in different time scales can be determined by running correlation analysis, so called Time Dependent Intrinsic Correlation (TDIC), proposed by Chen et al. [30]. The method is a data adaptive technique developed based on the Hilbert Huang Transform. In this method the following steps are involved:

1. Decompose the two associated time series using EEMD
2. Find the mean periodicities of components of the two series and identify the modes of similar periodicity
3. Perform HT of identified modes to obtain the instantaneous frequency (and hence instantaneous periods)
4. Fix the minimum sliding window size (t_d) as maximum instantaneous period between the two signals at the current position t_k, i.e., $t_d = \max(T_{1,i}(t_k), T_{2,i}(t_k))$ where $T_{1,i}$ and $T_{2,i}$ are instantaneous periods.
5. Estimate the size of sliding window as $t_w^{\,n} = \left[t_k - \frac{nt_d}{2} : t_k + \frac{nt_d}{2} \right]$

Where n is any positive number (a multiplication factor for minimum sliding window size) and normally n is selected as 1 [31]

6. Determine the correlation between the two modes for different sliding windows and estimate their statistical significance using *t*-test. Proceed iteratively till the boundary of the sliding window exceeds the end points of the time series

The results of TDIC analysis is obtained in the form of a TDIC matrix, and its plot will be triangular in shape, with time (the centre points of sliding window) in the horizontal axis and the size of the sliding window as vertical axis. The colorbar depicts the instantaneous correlation between the two modes. The correlation at the apex point will be the correlation coefficient between the modes considering the complete data length, if the data length is chosen as the maximum window size [30].

3. Study area and data set

Indian Institute of Tropical Meteorology (IITM) Pune defined five homogenous rainfall Zones in India such as North West India, Central India, West Central India, North East India and Peninsular India. The monthly rainfall data available from 1871 to 2017 for Peninsular India comprising of 6 subdivisions (Kerala, Tamilnadu, South Interior Karnataka, North Interior Karnataka, Coastal Karnataka, East Andhra Pradesh) covering 442908 sq.km are extracted from www.tropmet.res.in. Peninsular India is a region of unique geographical characteristics which covers the tropical wet and dry regions, with close proximity to Indian Ocean and Arabian sea and Bay of Bengal. Thus the role of large scale atmospheric circulations is primarily reflected in the monsoon characteristic of this region. The monthly (January - December) area weighted rainfall series for each of the 30 meteorological subdivisions have been prepared first in 1994 [32]. The SPI (McKee et al. 1993) is a meteorological drought index calculated using monthly precipitation values. A Gamma distribution is first fitted to the monthly precipitation values to compute the SPI. Subsequently, the distribution is converted to a standard normal distribution with variance equal to one and mean equal to zero, results the SPI values for the specified time scale. In this study, a monthly SPI dataset of SPI-3, SPI-6 and

SPI-12 are developed. To investigate the possible teleconnection of drought with the Indian Ocean Dipole (IOD) and ENSO, the IOD index and Nino index 3.4 of 146 years (1871-2016) has taken from https://www.esrl.noaa.gov.

4. Results and Discussion

The SPI index values of SPI-3, SPI-6 and SPI-12 is calculated from rainfall data of Peninsular India. The SPI indices are then decomposed using EEMD by selecting control parameters such as noise standard deviation, ensemble number and number of sifting iterations as 0.02, 100 and 10 respectively. The IOD index and Nino Index are also decomposed into IMFs using the same parameters. The EEMD package in MATLAB platform available at (http://perso.ens-lyon.fr/patrick.flandrin/eemd.html) is used for the above procedure after making necessary modifications. The EEMD of SPI-3 resulted in 10 IMFs and a residue, and that for SPI-6, SPI-12, IOD and Nino index resulted in 9 IMFs and a residue for each variable. The modes obtained by EEMD are presented in Fig.1.The basic properties of the modes obtained are analyzed in detail. The mean period of each of the signals are calculated by counting the number of zeroes and extrema. The mean period of modes, % variability explained by different modes are presented in Table 1.

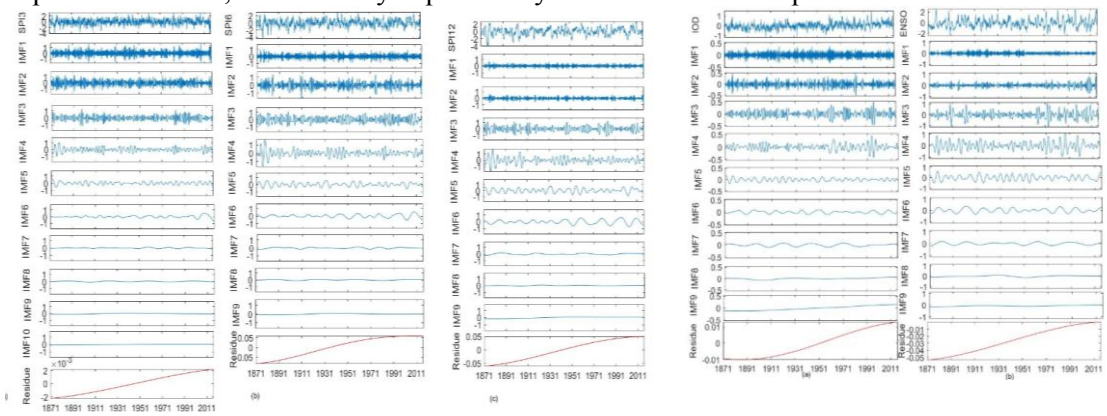

Figure 1 Orthogonal modes of (a) SPI-3 (b) SPI-6 (c) SPI-12 (d) IOD and ENSO (1871-2016)

Table 1 The mean period (in years) and Percentage variability explained of modes of IOD, ENSO, SPI-3, SPI-6 and SPI-12. T is the mean period (in months) and PE is the percentage variability explained by mode

	IOD		ENSO		SPI 3		SPI 6		SPI12	
IMF number	T	PE	T	PE	T	PE	T	PE	T	PE
IMF1	3.07	14.78	2.92	3.08	2.92	22.17	2.97	9.78	3.01	3.33
IMF2	7.25	16.53	7.14	5.51	7.15	20.24	8.03	17.02	7.15	4.06
IMF3	15.36	16.66	15.73	16.75	14.18	12.32	16.10	16.32	18.49	17.43
IMF4	33.01	12.80	37.59	20.39	28.74	9.07	32.95	15.19	36.22	21.50
IMF5	61.80	4.73	72.17	9.57	58.60	4.12	65.37	6.85	71.55	11.05
IMF6	140.65	2.82	138.21	5.28	116.56	2.65	126.56	4.57	150.43	9.28
IMF7	279.82	2.17	267.30	1.65	189.63	0.37	221.50	0.64	342.88	0.79
IMF8	770.33	1.00	669.50	0.58	434.80	0.24	459.80	0.20	454.75	0.12
IMF9	LT	0.33	LT	8.07	LT	0.40	LT	0.36	967.00	0.70
IMF10/Residue	LT	0.05	LT	0.06	LT	0.15	LT	0.23	LT	0.14
Residue						0.00018				

Note: LT = Long Term

From Table1, it is noted that IMF1 of all variables are having a process scale of 2.92-3.07 years which exhibits QBO with period ranging from two years to four years approximately. Similarly,

IMF2 show the periodicities close to phenomena ENSO which occur periodically varying from 4 to 10 years.

4.1 IOD teleconnections with the three SPI indices

To investigate the link between IOD and drought indices of Peninsular India, first the correlation between the modes of IOD and that of SPI-3, SPI-6 and SPI-12 are computed are presented in Table 2(a), (b) and (c) respectively. From Table 2 it is clear that the IOD and with the three SPI indices are strongly correlated in the higher order IMFs that represents a low frequency mode. Though it is a typical character of climatic teleconnections, one cannot ignore the strong association between them. Also, eventhough the overall correlation between the modes at other time scale are found to be small, the possibility of strong correlations at different localized time spells cannot be ignored. Therefore, to unmask such associations, the TDIC analysis is performed.

Table 2 Correlation between modes of IOD and modes of SPI. The bold numbers show statistically significant correlation

(a) Correlation between modes of IOD and modes of SPI-3

Modes of SPI3	IMF1	IMF2	IMF3	IMF4	IMF5	IMF6	IMF7	IMF8	IMF9	IMF10	Residue
IMF1	0.001	0.031	0.030	-0.003	-0.012	-0.005	-0.010	-0.011	-0.011	-0.002	0.003
IMF2	0.020	0.033	-0.054	0.014	0.018	-0.007	-0.014	-0.004	0.001	-0.002	-0.005
IMF3	-0.003	-0.005	0.047	-0.003	-0.004	0.002	0.01	0.020	0.001	0.012	0.014
IMF4	0.002	0.023	0.018	0.092	0.043	-0.008	-0.03	0.009	0.008	0.002	0.0004
IMF5	-0.0005	-0.0009	0.004	0.031	0.140	-0.002	-0.001	0.006	0.006	-0.004	-0.003
IMF6	-0.017	0.007	-0.007	0.011	-0.029	0.113	-0.057	0.004	-0.050	-0.057	-0.065
IMF7	0.0005	-0.006	0.015	-0.011	0.002	-0.010	-0.205	-0.001	-0.035	-0.046	-0.003
IMF8	-0.007	-0.006	0.007	-0.014	-0.002	0.056	-0.183	0.258	0.170	0.497	0.627
IMF9	-0.010	-0.004	-0.002	0.002	-0.035	0.064	-0.107	0.019	**0.261**	**0.902**	**0.990**
Residue	-0.011	-0.005	-0.002	0.001	-0.034	0.059	-0.099	0.007	**0.225**	**0.897**	**0.987**

(b) Correlation between modes of IOD and modes of SPI-6

Modes of SPI6	IMF1	IMF2	IMF3	IMF4	IMF5	IMF6	IMF7	IMF8	IMF9	Residue
IMF1	-0.071	-0.015	0.010	0.010	0.013	0.0005	-0.005	-0.004	-0.008	0.0004
IMF2	-0.027	-0.123	-0.034	-0.017	0.005	-0.011	-0.018	-0.012	-0.001	-0.003
IMF3	-0.013	-0.081	-0.116	0.018	-0.015	-0.007	0.007	0.013	0.001	0.013
IMF4	-0.008	-0.015	-0.045	-0.064	0.085	-0.009	-0.008	0.009	0.007	0.001
IMF5	-0.002	0.019	0.023	0.0002	-0.181	-0.013	-0.024	0.011	0.001	-0.004
IMF6	-0.001	0.010	0.0004	-0.018	-0.076	0.093	0.003	-0.022	-0.059	-0.060
IMF7	-0.010	0.003	-0.002	-0.005	-0.031	0.035	-0.121	0.180	-0.016	-0.030
IMF8	-0.003	0.002	-0.006	0.012	0.032	0.036	-0.042	0.461	**0.282**	**0.557**
IMF9	0.007	0.010	-0.023	0.017	0.001	0.042	0.061	0.103	**0.404**	**0.953**
Residue	0.008	0.011	-0.022	0.016	-0.001	0.038	0.061	0.066	**0.364**	**0.950**

(c) Correlation between modes of IOD and modes of SPI-12

Modes of SPI 12	IMF1	IMF2	IMF3	IMF4	IMF5	IMF6	IMF7	IMF8	IMF9	Residue
IMF1	-0.035	-0.001	0.011	0.006	0.014	-0.0009	-0.005	-0.009	-0.003	0.002
IMF2	-0.030	-0.060	-0.031	0.002	0.0003	-0.013	-0.015	-0.006	-0.002	-0.004
IMF3	0.013	0.008	0.025	-0.023	-0.009	-0.012	0.009	0.016	0.010	0.014
IMF4	0.005	0.013	-0.120	-0.107	0.100	-0.024	0.006	0.009	0.004	0.001
IMF5	0.0002	-0.004	-0.024	-0.046	-0.104	0.027	-0.001	0.023	-0.001	-0.003
IMF6	0.001	0.001	-0.032	-0.008	0.019	0.121	-0.050	-0.048	-0.067	-0.063
IMF7	0.006	0.003	0.008	0.004	-0.019	-0.062	0.126	0.130	-0.030	-0.015
IMF8	-0.004	-0.009	0.005	0.011	0.047	-0.011	0.189	**0.467**	**0.493**	**0.600**
IMF9	-0.001	-0.009	-0.015	0.015	0.014	0.020	0.123	0.221	**0.823**	**0.979**
Residue	-0.001	-0.008	-0.014	0.013	0.011	0.017	0.116	0.192	**0.806**	**0.977**

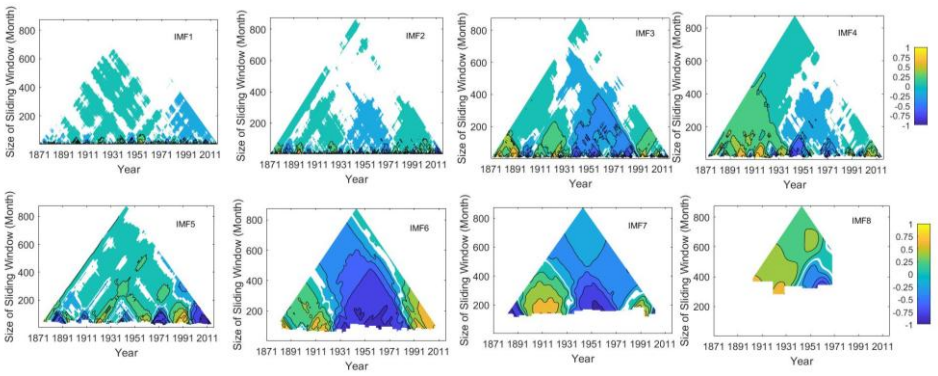

Figure 2 TDIC plots of modes of IOD index and SPI-3

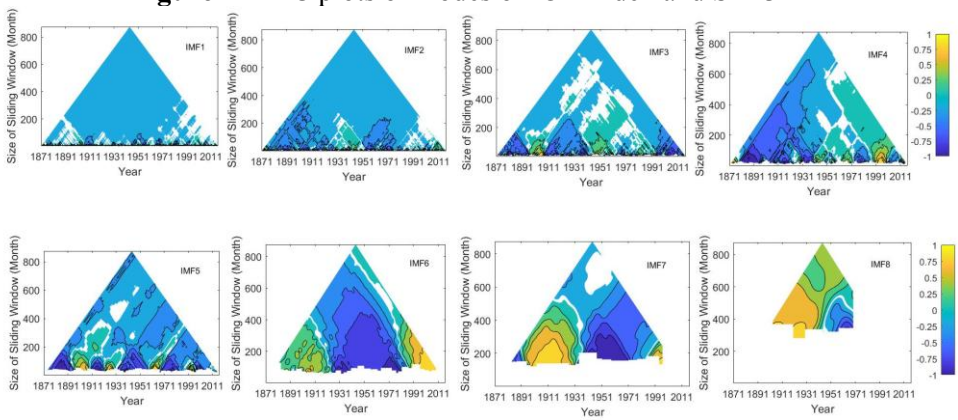

Figure 3 TDIC plots of modes of IOD index and SPI-6

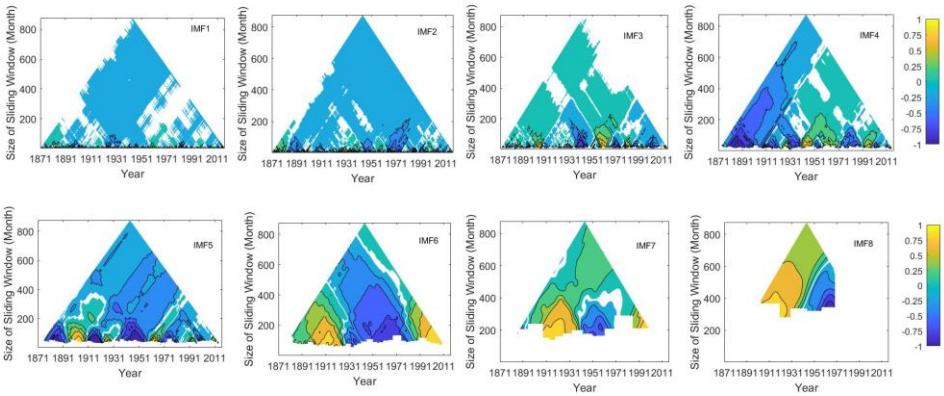

Figure 4 TDIC plots of modes of IOD index and SPI-12

A one to one IMF TDIC analysis is performed (i.e., the association between IMF1 of IOD and IMF1 of SPI-3). From TDIC plots, it can be inferred that the association between IOD and drought indices are of different nature in different process scales. Weakly positive association is dominant in most of the IMFs in Fig 2. In IMF6 and IMF7 some localized positive associations are seen in different time spells though negative association is predominant in both of them. Strong relations are seen in nineteenth century, the period which has many drought years. The SPI-6 relation to IOD (Fig. 3) exhibits negative relation prevalent from IMF1 to IMF7. Localized positive associations are seen in especially in IMF6 and IMF7. Among the IMFs obtained in Fig 4 SPI-12 and IOD relation showcases strong negative association in IMF1, IMF2 and IMF5 while positive dominancy exists over IMF3 and IMF4. IMF6 exposes partially positive and negative correlations

between SPI12 and IOD. IMF7 exhibits strong positive correlation in the entire period which is an influencing IMF for the prediction of drought.

Comparing the three SPI indices, SPI-3 is preferred over the other two. Though some of the modes of SPI-6 and SPI-12 experience positive correlation with IOD, the evidence of strong positive association between SPI-3 and IOD makes it more prominent index in relation to the prediction of drought years. Apart from the fact that SPI-12 gives higher correlation coefficients than SPI-6, the values from Table 2 also supports that SPI-3 could achieve even better correlation coefficients than SPI-12. In addition to that, IMF7 of SPI-12 can be used to get further accurate predictions.

4.2 ENSO teleconnections with the three SPI indices

As the ENSO influences temperature and precipitation, which in turn affects the rainfall pattern, it is appreciable to discover the link between ENSO and drought indices of Peninsular India. Accordingly, the correlation between the modes of ENSO and that of SPI-3, SPI-6 and SPI-12 are computed are presented in Table 3. Low frequency modes show strong association between ENSO and drought indices. TDIC analysis is executed to capture profound information.

Table 3 Correlation between modes of ENSO and Modes of SPI series

(a) Correlation between modes of ENSO and modes of SPI-3

Modes of SPI 3	IMF1	IMF2	IMF3	IMF4	IMF5	IMF6	IMF7	IMF8	IMF9	IMF10	Residue
IMF1	-0.009	-0.002	0.001	0.006	0.0001	-0.006	-0.004	0.001	0.006	0.001	-0.001
IMF2	0.007	0.042	0.025	0.027	0.033	0.041	0.026	0.024	0.019	-0.004	-0.018
IMF3	-0.006	0.049	0.107	0.201	0.059	0.001	-0.002	0.005	0.010	0.002	0.0005
IMF4	-0.016	0.012	0.022	0.209	0.126	-0.037	-0.014	-0.025	0.002	-0.007	-0.004
IMF5	-0.027	-0.010	0.008	0.092	0.023	-0.171	-0.012	-0.015	0.016	0.019	0.01-
IMF6	-0.001	-0.007	0.009	0.009	-0.038	0.027	0.218	-0.063	0.004	0.017	0.020
IMF7	0.002	-0.009	-0.006	0.005	-0.038	-0.054	0.214	0.130	0.004	-0.037	-0.056
IMF8	-0.008	0.011	-0.006	0.017	-0.022	0.004	0.041	-0.081	0.048	**0.311**	**0.375**
IMF9	-0.006	0.006	-0.002	0.012	-0.042	0.066	-0.076	-0.046	0.084	**0.647**	**0.782**
Residue	-0.012	-0.003	-0.004	0.009	-0.043	0.056	-0.076	-0.016	**0.369**	**0.958**	**0.998**

(b) Correlation between modes of ENSO and modes of SPI-6

Modes of SPI 6	IMF1	IMF2	IMF3	IMF4	IMF5	IMF6	IMF7	IMF8	IMF9	Residue
IMF1	0.039	-0.001	-0.002	0.004	-0.002	-0.005	-0.001	0.001	0.004	0.0001
IMF2	-0.005	-0.010	-0.066	-0.008	0.023	0.016	0.011	0.002	0.011	-0.010
IMF3	-0.020	-0.071	-0.231	-0.101	-0.008	-0.016	-0.004	0.008	0.010	0.001
IMF4	-0.005	0.001	-0.054	-0.199	-0.204	-0.036	-0.003	0.002	0.008	-0.006
IMF5	-0.007	0.005	0.017	0.019	-0.300	-0.136	0.015	-0.013	0.017	0.018
IMF6	-0.008	-0.007	0.001	0.014	-0.051	0.157	0.194	-0.046	0.012	0.018
IMF7	-0.006	0.011	-0.007	-0.012	-0.037	0.086	0.070	-0.020	-0.014	-0.045
IMF8	-0.004	0.002	-0.023	0.018	-0.014	0.037	0.105	-0.095	0.097	**0.345**
IMF9	0.0006	0.005	-0.027	0.024	-0.007	0.058	0.124	0.031	**0.238**	**0.714**
Residue	0.007	0.011	-0.024	0.018	-0.008	0.037	0.079	0.062	**0.499**	**0.989**

(c) Correlation between modes of ENSO and modes of SPI-12

Modes of SPI-12	IMF1	IMF2	IMF3	IMF4	IMF5	IMF6	IMF7	IMF8	IMF9	Residue
IMF1	0.026	0.013	0.004	-0.003	-0.0002	-0.004	-0.004	0.003	0.002	-0.001
IMF2	0.004	0.048	-0.046	-0.011	0.015	0.008	-0.009	-0.005	-0.001	-0.014
IMF3	0.009	0.0002	-0.277	-0.147	-0.019	-0.010	-0.004	0.008	0.005	0.001
IMF4	0.008	0.012	-0.152	**-0.331**	-0.200	-0.031	0.008	-0.0003	-0.002	-0.006
IMF5	-0.0002	0.0001	-0.010	-0.081	-0.251	-0.072	0.009	0.003	0.019	0.016
IMF6	-0.0008	0.0009	-0.001	0.037	-0.055	0.141	0.063	-0.023	0.015	0.018
IMF7	0.0005	-0.001	-0.004	0.007	-0.066	0.105	0.082	-0.040	-0.038	-0.052
IMF8	0.007	-0.002	-0.009	0.022	0.009	0.016	-0.017	-0.001	0.253	0.358
IMF9	0.003	-0.007	-0.026	0.028	0.012	0.038	0.118	0.108	**0.561**	**0.749**
Residue	0.0003	-0.009	-0.018	0.017	0.005	0.021	0.109	0.231	**0.889**	**0.999**

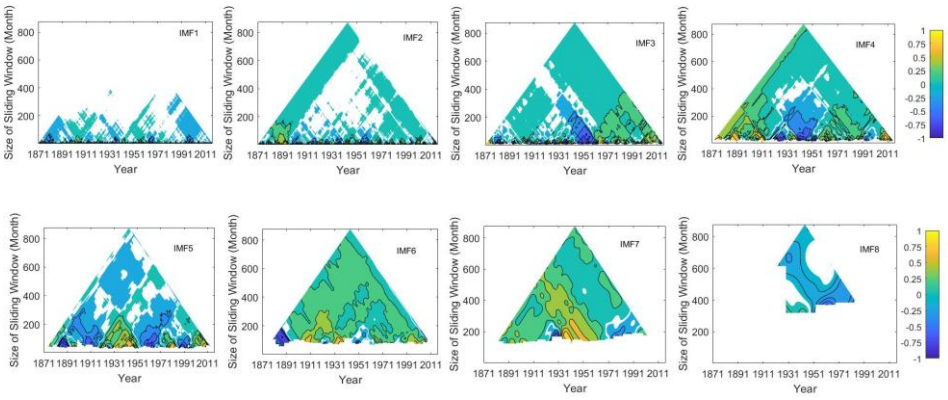

Figure 5 TDIC plots of modes of ENSO and SPI-3

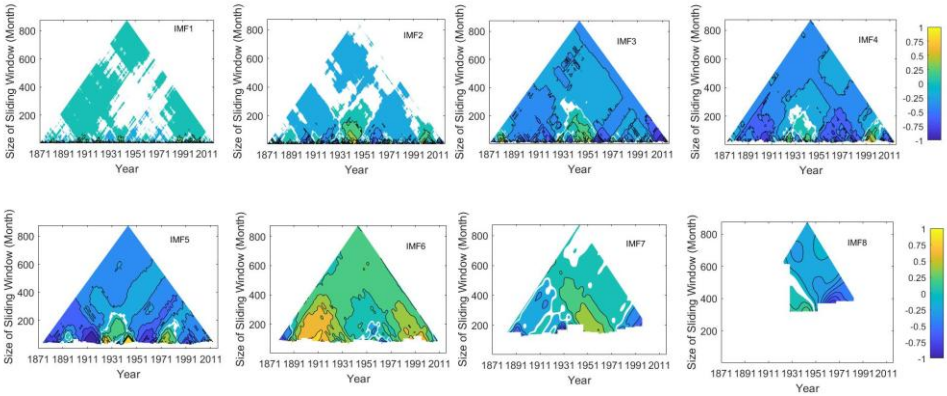

Figure 6 TDIC plots of modes of ENSO and SPI-6

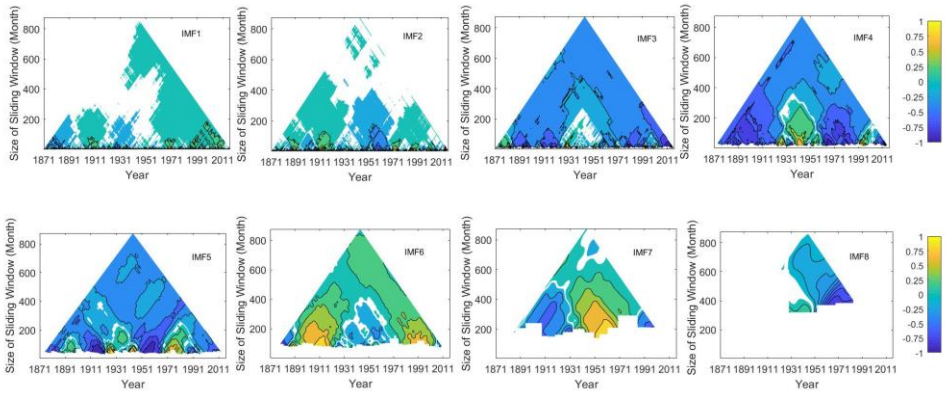

Figure 7 TDIC plots of modes of ENSO and SPI-12

The relation between SPI-3 and ENSO (Fig 5) exhibits positive correlation in IMF2, IMF3 and IMF4 and stronger relation in IMF6 and IMF7.IMF5 shows highly negative association. Therefore, IMF5 is an irrelevant factor for drought prediction. Most of the IMFs in Fig 6 shows a negative dominancy in SPI-6 –ENSO teleconnection. Only IMF6 retains a positive correlation. IMF1 and IMF2 though show positive correlation most of the values does not satisfy 95% confidence interval in Fig 7. Strong negative association is seen in IMF3, IMF4 and IMF5. Though some localized negative associations exist in IMF7, the presence of more positive associations in IMF6 and IMF7 make them a reliable process scale for further studies.

From the TDIC plots (Fig 2 and Fig 5), high frequency modes possess similar positive correlation to SPI-3. Comparing Fig 3 and Fig 6 IMF1 to IMF5 trails opposite correlations for IOD and ENSO while for IMF6 and IMF7 show a similar nature (of positive correlation). In Fig 4 and Fig 7, IOD and ENSO exhibits characteristics opposite to each other in relation to drought indices for IMFs, except IMF5 in which both shows negative tendency of correlation. Ashok et al., [33] states that the IOD influences association between the ENSO and monsoon rainfall thereby drought. The results indicate that there is a lagged influencing relation between IOD and ENSO that promotes correlation between rainfall and ENSO.

5. Conclusions

This study proposed the application of TDIC method for investigating the multiscale teleconnection of drought indices of Peninsular India. The results show that IOD and ENSO influences the short term drought (SPI-3) in a better way than other long or medium drought indices. Against the recognized negative correlation of IMFs of medium and long drought indices, it is well identified that the Indian monthly drought can be modelled in a better way using IMF3 and IMF7 of SPI-12, inaddition to the existing knowledge captured from short term drought IMFs of IOD. Concurrently, The Analysis also establishes an evidence of drought-ENSO teleconnections that includes the fact that concurrent effects of IMF2 to IMF7 of SPI-3, IMF1, IMF6 and IMF7 of SPI-6, and IMF6 and IMF7 of SPI-12 may improve the efficacy of prediction and helps to determine the severity with respect to ENSO. Also, the TDIC analysis obtained reveal that the short term drought is more linked to IOD in high frequency modes while the drought predictability factor for ENSO is more positively correlated to low frequency intrinsic mode functions.

Acknowledgments

Authors are grateful to the Indian Institute of Tropical Meteorology Pune for providing the relevant data regarding rainfall in the public domain. The authors also thank National Oceanic and Atmospheric Administration for making available data regarding ENSO and IOD indexes for research. The authors also thank Department of Computer Science and IT, Amrita School of Arts and Sciences for the support provided.

References

[1] McKee T B, Doesken N J and Kleist J 1993 The relationship of drought frequency and duration to time scales. *In Proceedings of the 8th Conference on Applied Climatology, AMS: Boston* **17** 179-183

[2] Palmer W C 1965 Meteorological drought. Research paper no. 45. *US Weather Bureau Washington* **58**

[3] Hayes M, Svoboda M, Wall N and Widhalm M 2011 The Lincoln declaration on drought indices: universal meteorological drought index recommended. *B Am Meteorol Soc* **92** 485-88

[4] Vicente-Serrano SM, Beguería S and López-Moren J-I 2010 A Multiscalar Drought Index Sensitive to Global Warming: The Standardized Precipitation Evapotranspiration Index. *J. Climate* **23** 1696-1718

[5] Walker GT 1923 Correlation in seasonal variations of weather VIII, A preliminary study of world-weather. *Memoirs Indian Met Dept* **24** 75-131

[6] Krishna Kumar KB, Rajagopalan B and Cane M A 1999 On the weakening relationship between the Indian monsoon and ENSO. *Science* **284** 2156-59

[7] Kumar KK, Rajagopalan B, Hoerling M, Bates G and Cane M 2006 Unraveling the mystery of Indian monsoon failure during ElNiño. *Science* **314** 115-9

[8] Goswami BN, Madhusoodanan MS, Neema CP and Sengupta D 2006 A physical mechanism

for North Atlantic SST influence on the Indian summer monsoon. *Geophys. Res.* 33 L02706, doi:10.1029/2005GL024803.

[9] Gadgil S, Vinayachandran PN, Francis PA and Gadgil S 2004 Extremes of the Indian summer monsoon rainfall, ENSO and equatorial Indian Ocean oscillation. *Geophys. Res.* **31** L12213 doi:10.1029/2004GL019733

[10] Saji NH, Goswami BN, Vinayachandran and Yamagata T 1999 A dipole mode in the tropical Indian Ocean. *Nature* **401** 360–3

[11] Vinayachandran P N, Francis P A and Rao S A 2009 Indian Ocean dipole: processes and impacts. *Current trends in science* 569-89

[12] Bala I and Singh OP 2008 Relationship between Indian Ocean dipole and summer monsoon. Mausem **59** 167-172

[13] Johny K, Pai M and Adarsh S 2018 Empirical forecasting and Indian Ocean dipole teleconnections of south–west monsoon rainfall in Kerala. *Meteorol Atmos Phys* 1-11. doi: 10.1007/s00703-018-0620-7

[14] Krishnamurthy V and Goswami B N 2000 Indian monsoon–ENSO relationship on interdecadal timescale. *J. Clim.* **13** 579-595

[15] Kripalani RH and Kulkarni A 1997a Climatic impacts of El Niño/La Nina on the Indian monsoon: A new perspective. *Weather* **52** 39– 46

[16] Kripalani RH and Kulkarni A 1997b Rainfall variability over south East Asia- Connections with Indian monsoon and ENSO extremes: New perspectives. *Int J Climatol* **17** 1155-68

[17] Valcárcel A R 2018 Teleconnections between ENSO and rainfall and drought in Puerto Rico. *Int J Climatol.* **38** e1190-e1204.

[18] Rashid M M, Johnson F and Sharma A 2018 Identifying sustained drought anomalies in hydrological records: A wavelet approach. *J. Geophys. Res: Atmos.* **123** 7416-32

[19] Abiy A Z, Melesse A M and Abtew W 2019 Teleconnection of Regional Drought to ENSO, PDO, and AMO: Southern Florida and the Everglades. *Atmosphere* **10** 295

[20] Ashok K and Saji N H 2007 On the impacts of ENSO and Indian Ocean dipole events on sub-regional Indian summer monsoon rainfall. *Nat Hazards* **42** 273-285

[21] Narasimha R and Bhattacharyya S 2010 A wavelet cross-spectral analysis of solar–ENSO–rainfall connections in the Indian monsoons. *Appl Comput Harmon A.* **28** 285-95

[22] Gaughan A E, Staub C G, Hoell A, Weaver A and Waylen P R 2016 Inter and Intra annual precipitation variability and associated relationships to ENSO and the IOD in southern Africa. *Int J Climatol.* **36** 1643-56

[23] Araghi A, Mousavi- Baygi M, Adamowski J and Martinez C 2017 Association between three prominent climatic teleconnections and precipitation in Iran using wavelet coherence. *Int J Climatol.* **37** 2809-30

[24] Maity R and Nagesh Kumar D 2006 Bayesian dynamic modeling for monthly Indian summer monsoon rainfall using El Nino–Southern Oscillation (ENSO) and Equatorial Indian Ocean Oscillation (EQUINOO). *J. Geophys. Res. Atmos* **111**

[25] Maity R, Kumar D N and Nanjundiah R S 2007 Review of hydroclimatic teleconnection between hydrologic variables and large-scale atmospheric circulation patterns with Indian perspective. *ISH J. Hydraul. Eng.* **13** 77-92

[26] Adarsh S and Janga Reddy M 2016 Analysing the hydroclimatic teleconnections of summer monsoon rainfall in Kerala, India using Multivariate Empirical Mode Decomposition and time dependent intrinsic Correlation. *IEEE Geosci Remote* S **13** 1221-25

[27] Adarsh S and Janga Reddy M 2017 Multiscale characterization and prediction of monsoon rainfall in India using Hilbert–Huang transform and time-dependent intrinsic correlation analysis. *Meteorol Atmos Phys.* **130** 667-8

[28] Huang NE, Shen Z, Long SR, Wu MC, Shih HH, Zheng Q, Yen NC, Tung CC and Liu HH 1998 The empirical mode decomposition and the Hilbert spectrum for nonlinear and non-stationary time series analysis. *P Roy Soc A-Math Phy* **454** 903-995

[29] Wu Z and Huang NE 2005 Ensemble empirical mode decomposition: A noise-assisted data analysis method. *Cent. for Ocean-Land-Atmos. Stud., Calverton, Md* 1-51 (ftp://grads.iges.org/pub/ctr/ctr_193.pdf)
[30] Chen X, Wu Z and Huang NE 2010 The time-dependent intrinsic correlation based on the empirical mode decomposition. *Adv Adapt Data Anal* **2** 233–65
[31] Huang Y and Schmitt FG 2014 Time dependent intrinsic correlation analysis of temperature and dissolved oxygen time series using empirical mode decomposition. *J Marine Syst* **130** 90–100
[32] Parthasarathy B Munot AA and Kothawale DR 1994 All-India monthly and seasonal rainfall series: 1871–1993. *Theor Appl Climatol* **49** 217–24
[33] Ashok K, Guan Z and Yamagata T 2001 Impact of the Indian Ocean dipole on the Relationship between the Indian monsoon rainfall and ENSO. *Geophys. Res.***28** 4499-4502